

High Resolution Mapping of a Fast Spreading Mid Ocean Ridge with the Autonomous Benthic Explorer

Dana R. Yoerger¹, Albert M. Bradley², Marie-Helene Cormier³,
William B. F. Ryan⁴, Barrie B. Walden⁵

Abstract

The Autonomous Benthic Explorer (ABE) of the Woods Hole Oceanographic Institution acquired an extremely high resolution near-bottom multisensor dataset along and across the narrow neovolcanic and active tectonic zone of the southern East Pacific Rise (17°-19°S). Exploiting its abilities for precise navigation, trackline following, and bottom-following in rough terrain, ABE collected bathymetry, magnetics, temperature, optical backscatter, conductivity, and digital video imaging. The dives were conducted at a depth of approximately 2600 meters over 19 individual nighttime deployments from the RV Atlantis.

1. Introduction

In February 1999, we utilized the the Autonomous Benthic Explorer (ABE) of the Woods Hole Oceanographic Institution to obtain a high-resolution data set on the southern East Pacific Rise, working near the seafloor over rugged volcanic terrain at depths of 2600 meters. ABE's capabilities for precise navigation and control were exploited to produce a multisensor data set that revealed fine-scale details of the seafloor.

ABE can survey the near-bottom environment at depths to 5000 meters with a variety of sensors (figure 1). ABE's ability to maneuver independently in all three translational axes and heading at any speed makes it unique among the current crop of AUVs in use for science.

Our early deployments concentrated on precisely navigated magnetometer surveys over extremely rugged terrain around active crustal spreading regions [1]. In these earlier efforts, we demonstrated ABE's ability to follow pre-programmed tracklines using long-baseline acoustic navigation and terrain-follow over difficult terrain including steep scarps. For the southern East Pacific Rise work, we added a scanning sonar to our vehicle to enhance the cross-track bathymetric coverage.

In our proposed program, we planned a series of zig-zag patterns across the ridge axis, collecting magnetometer data with the bathymetric data as a secondary product. However, we found we could produce a much superior data set for both magnetics and bathymetry by programming ABE to follow closely-spaced (15-40 meter) parallel tracks to provide complete coverage with the scanning sonar.

¹ Associate Scientist, Woods Hole Oceanographic Institution, email: dyoerger@whoi.edu

² Principal Engineer, Woods Hole Oceanographic Institution, email: abradley@whoi.edu

³ Associate Research Scientist, Lamont-Doherty Earth Observatory, email: cormier@ldeo.columbia.edu

⁴ Doherty Senior Scientist, Lamont-Doherty Earth Observatory, email: billr@ldeo.columbia.edu

⁵ Principal Engineer, Woods Hole Oceanographic Institution, email: bwalden@whoi.edu

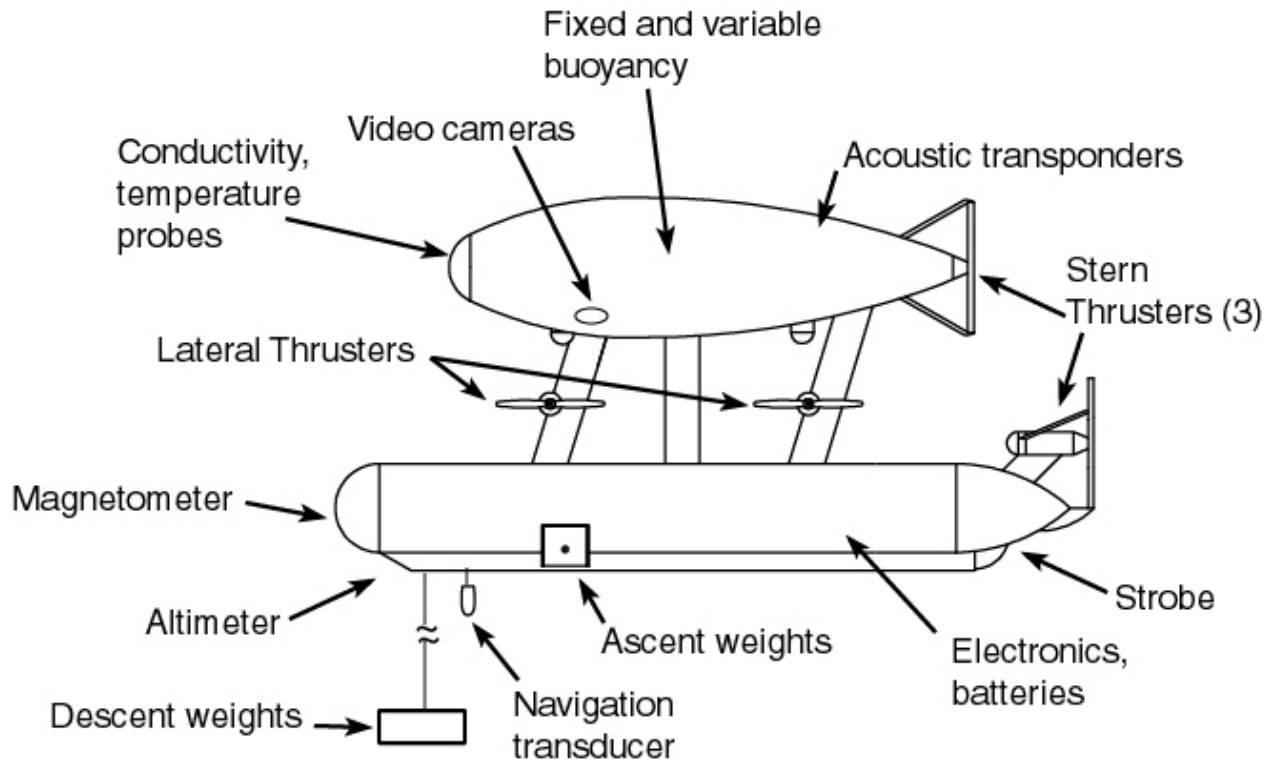


Figure 1. The Autonomous Benthic Explorer (ABE) is propelled by 7 thrusters and can maneuver in any direction or change heading over its entire operating range. A descent weight on a short mooring carries ABE to the seafloor, and it returns to the surface when the ascent weights have been released.

After building a bathymetric map, we programmed ABE to track along specific features at a height appropriate for ABE's electronic video snapshot system. From these runs, we built stereo renderings and photomosaics coregistered with bathymetry. Additionally, ABE detected a number of active hydrothermal vents by concurrent readings on the conductivity, temperature, optical backscatter, and video snapshot sensors. Finally, ABE collected samples of volcanic glass using a wax coring technique.

1.1 Cruise Plan & ABE Operation

We met Atlantis in late January 1999 at Easter Island. ABE had been shipped to Manzanillo, Mexico in a 20 ft container and loaded onto the vessel several months earlier, as Easter Island's rudimentary port facilities provide access to the vessel only by small boat. We reached the dive site after a two day transit. Following the deployment and survey of transponders, we began several days of sonar survey with the DSL-120 sidescan system, then started daytime Alvin operations and a nighttime program consisting of wax coring, dredging, and ABE operations. We executed 19 ABE dives, then transited 6 days to Manzanillo, where all gear was offloaded.

We had significant departures from the intended ABE dive plan early in the cruise. Our first dive returned no science data due to failure of the gyro compass and long baseline acoustic navigation. We also had two aborted dives when the vehicle experienced high shock loads on launch. All remaining

dives returned useful science data, although some of the early dives ended prematurely due to battery problems. Improper rejection of acoustic surface-bounce returns corrupted navigation and prevented ABE from following the correct track on several other dives.

Eventually we settled into a routine where we would launch ABE about 1830 and schedule it to come back to the surface at 0530 before first light, which allowed us to easily spot its strobes. We would have ABE on deck by 0600 and immediately begin downloading and postprocessing data. We plotted the maps from the night's run within a few hours of ABE's return. When an Alvin dive was conducted in an area where ABE had surveyed the night before, we were able to provide a detailed map of the area before Alvin's launch at 0800. Our science team would spend the day reviewing the data and working up a plan for the next night. We would program the new dive, test it in simulation, and launch again at 1830.

ABE dives were conducted at night along with wax coring, which utilizes the vessel's cable and winch to pick up small samples of volcanic glass from the seafloor. For the early dives, we conducted the wax cores in positions that allowed us to monitor ABE's progress. But by the end of the cruise we were able to completely ignore ABE once launched and release the vessel to work without constraint.

1.2 Summary of Results

We surveyed three segments of the East Pacific Rise working from south to north. At the southernmost region we did open zig-zag patterns across the spreading axis. At the center section we tried close spaced parallel tracks providing overlapping bathymetric coverage of the bottom across a rift valley with steep sides. Our most extensive data set was generated at the northernmost and last of the three regions surveyed. Here we spent each night's dive adding on to a growing area of contiguous bathymetric coverage plus doing special survey segments concentrating on low altitude video runs. For the sonar runs, ABE flew at 20 meters off the bottom and our sonar covered (45 degrees, giving a 40m swath. The sonar "pixels" on the bottom were spaced about every 2m cross track and 5m along track at our vehicle's 0.6m/s nominal survey speed. Video segments were run with the vehicle approximately 5 meters off the bottom.

Below are the dive statistics for the cruise:

- * total dives: 20
- * dives yielding science data: 17
- * total distance traveled on the bottom: 110.25 km
- * total bottom time: 55:21:37
- * total number of video snapshots: 6929
- * area surveyed with scanning sonar: approximately 3.3 km²
- * longest dive: 12.1 km on bottom

2. Navigation and Control

ABE uses acoustic travel times from a network of up to 4 transponders moored to the seafloor to determine its position during its descent and while surveying. Before the first vehicle launch, we survey in the transponders by interrogating them from vessel positions known from pcode GPS. The

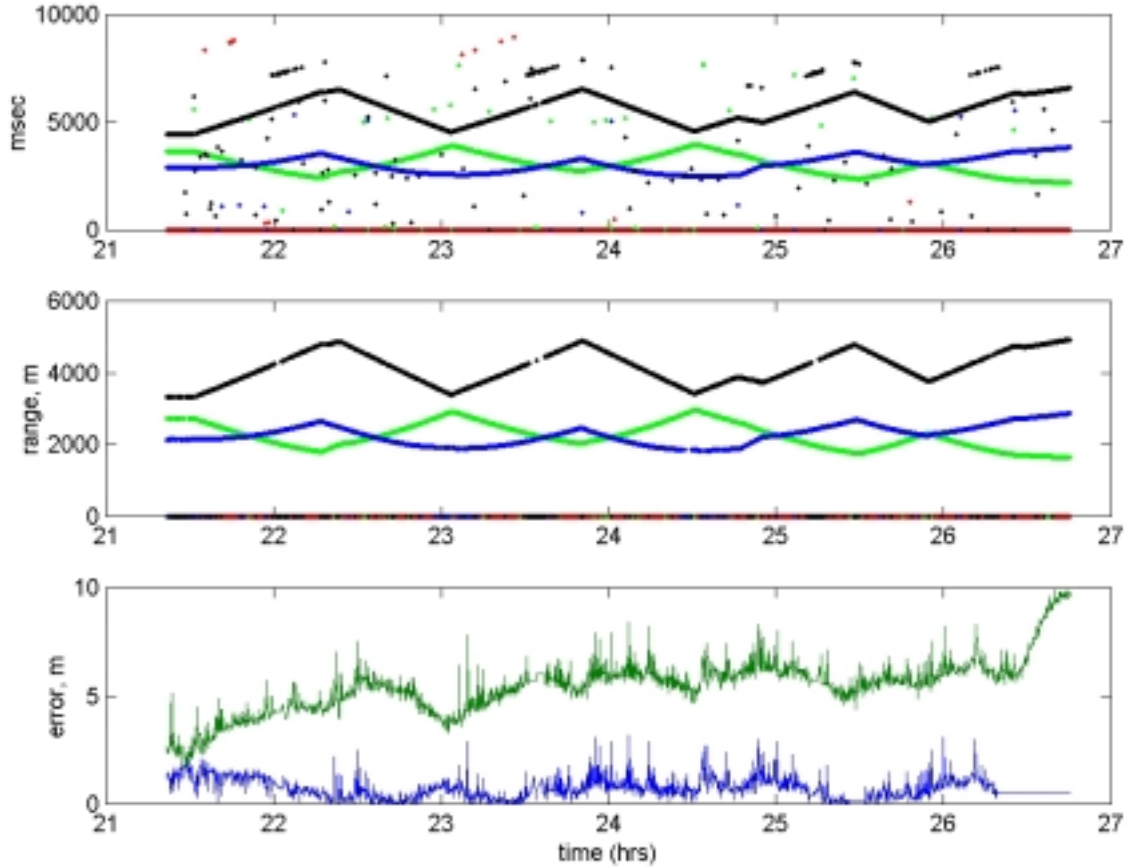


Figure 2. The upper plot shows raw transponder travel-times received at the vehicle. Random bad returns (caused by noise) as well as systematic bounce-path returns can be seen. The second plot shows the horizontal range estimates after median filters and range gates were applied. The lower plot shows RMS range error before and after the transponder positions were corrected using data gathered at the vehicle.

position fixes allow ABE to control its descent and to follow tracklines with precision. After recovering the vehicle we further process the data, recovering fixes that were rejected in real-time and refining the transponder survey by using the returns received at the vehicle.

2.1 Long Baseline Navigation Algorithm

The hardware and algorithms used for this effort were similar to those used in our 1996 dives [1,2] with two significant refinements. First, we improved our ability to reject surface bounces by dynamically changing the transponder range gates. Second, we used data from the vehicle's in-hull navigation between dives to refine the transponder survey for subsequent runs. By improving survey quality, we improved agreement between fixes computed from different combinations of transponders.

The long baseline navigation algorithm works as follows:

1. Travel-times are converted to ranges and projected into the horizontal plane using the vehicle depth measurement.
2. Ranges are checked with median filters (for consistency) and range gates (to eliminate bounce paths)
3. If three or more good ranges have been received, the algorithm computes a 2D least-squares solution.
4. If the rms range residual is less than a preset minimum, then the fix is accepted. If not, the range that disagrees most with the last good fix is eliminated and the fix computation repeated.
5. If only two good ranges have been received, the algorithm computes a deterministic 2D solution, with the baseline side chosen according to the estimated position from the previous time step. If the geometry is poor for a proper 2D solution, the fix is rejected.
6. The previous position estimate is propagated forward using an estimate of the vehicle speed and the vehicle heading.
7. If a good fix has been received, the estimate and the fix are blended using a first-order estimator.

The dynamic adjustment of the range gates involved altering the maximum acceptable travel time for each trackline segment. Previously, we set a maximum range for each transponder based on the minimum expected surface bounce path over the entire survey area. For the trackline lengths (3 km) implemented on this survey at the operating at 2600 meters, the minimum bounce path length while closest to a transponder could be less than the direct path at the maximum distance from the transponder. Improper management of the range gates caused the navigation to accept surface bounce returns during the transition from descent to the first trackline on several early dives. We solved this problem by adjusting the gate for each trackline, or trackline segment for very long tracks. This was accomplished using our existing command set.

We also improved the quality of our transponder surveys using the in-hull travel-time data from ABE between dives. We used an iterative nonlinear minimization technique to systematically adjust the baseline lengths to reduce the RMS range error (the same metric that is minimized in the least-squares fix solution) averaged over the entire run. Using a direction-set technique [3], one-parameter minimizations were performed on each baseline length, then the entire sequence was repeated until convergence occurred. Typical adjustments ranged from 1 to 8 meters.

2.1 Navigation Results

Figure 2 shows the low-level performance of the navigation algorithm for the dive ABE 39, which took place in the northern area. The top plot shows the raw travel times detected at the vehicle. The second plot shows the range estimates determined by the real-time algorithm after the travel times had been converted to horizontal ranges and subjected to the range gates and median filters. The lower plot shows the RMS range residuals before and after the transponder survey was improved. Adjusting the transponder baseline lengths had a strong effect, dropping the average error from 5.45 meters to 0.74 meters on that particular run.

Such a reduction in the fix error has several crucial benefits. Lower error means that the overall navigation grid will contain less distortion. Additionally, fixes will jump less when the combination of transponders changes (for example when one of three transponders temporarily drop out). This

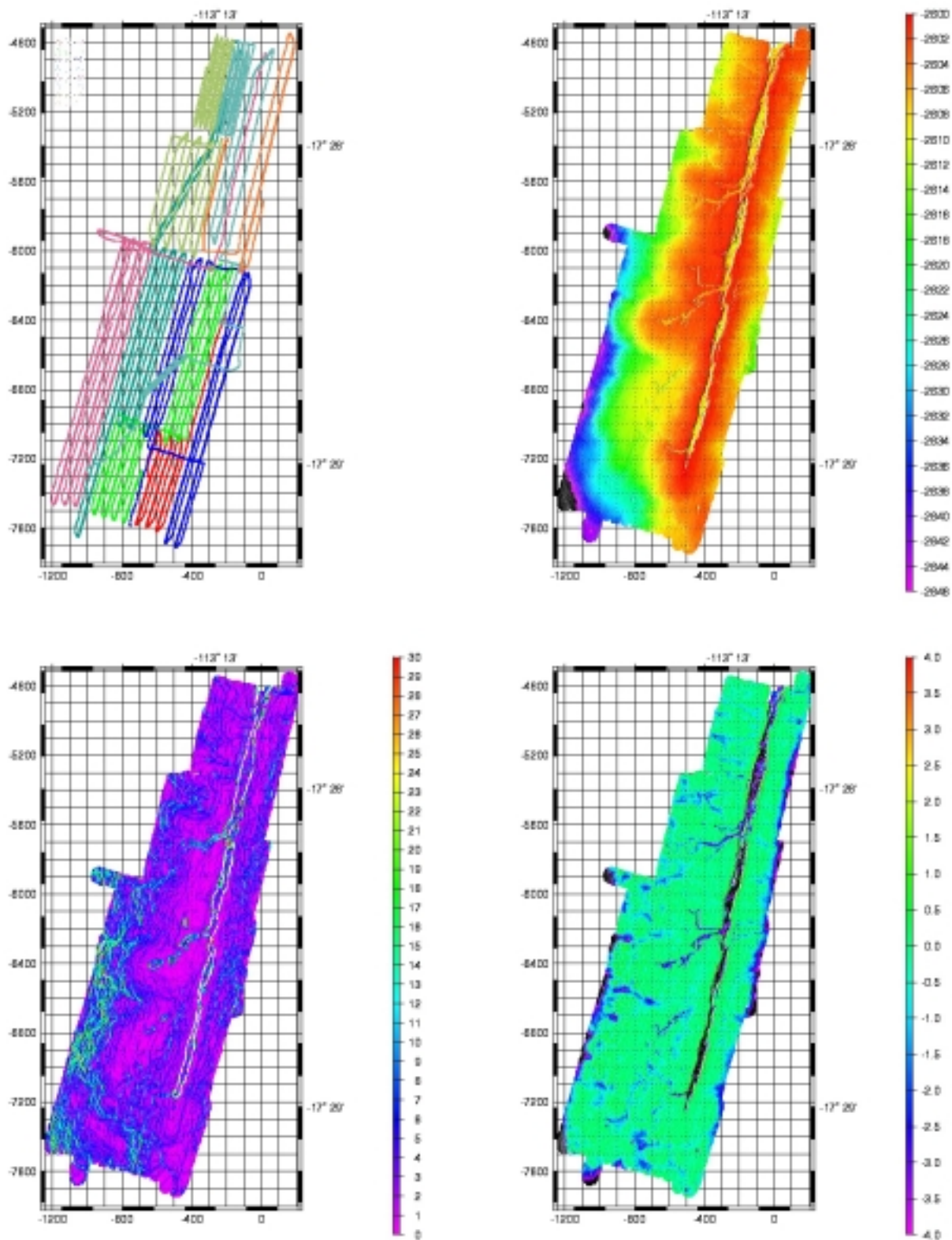


Figure 3. These plots show the results of the sonar microbathymetry in the northern area. The top left plot shows the vehicle tracklines for eight dives. The upper right plot shows shaded bathymetry, which includes a variety of geological features. The bottom two plots show the slope (left) and the relief (right), which are useful both for geological interpretation and illustrate the overall integrity of the data set.

results in smoother real-time control of the vehicle as well as improved post-processing of the sonar records.

3. Bathymetric Mapping with ABE

In post-processing, we transformed the range and bearing measurements from the scanning sonar into a “dot cloud” of points registered in world coordinates. For the type of data gathered in these surveys, where the depth can be assumed to be a function of horizontal position, standard gridding routines [4, 5] can be used to create a surface rendering. The sonar processing effort was greatly enhanced by the use of software developed to process data from the Jason ROV system[6,7]. This software had been used extensively for archaeological mapping on the Skerki Bank cruise in 1997 [8] and the Edifice Rex effort also in 1997. Likewise, techniques for removing systematic biases in sensor data were also borrowed directly from the earlier Jason efforts.

3.1 Methodology

First, the navigation was reprocessed to increase the number of fixes, reduce errors, and produce a smooth output that dynamically represented a plausible vehicle track. Transponder ranges were run through a double-sided median filter with manually adjusted range gating. These post-processing techniques allow more ranges to be utilized than the more conservative real-time filters. Then, the fixes were recomputed from the improved set of ranges when they were available. Finally, the fixes were transformed to the vehicle center of gravity, and an acausal smoothing filter was applied.

ABE’s heading was measured by a fluxgate compass and a rate gyro. Principal errors include the rate offset in the gyro and nonuniformity in the mapping between the measured fluxgate reading and the true heading. The vehicle heading was corrected utilizing the redundancy between the flux gate and rate gyro using data from the descent phase when the vehicle was far from magnetic anomalies (the vessel or the seafloor). The rate gyro has an offset that is nonzero but very stable. The offset could be deduced by comparing the integrated rate gyro signal to the fluxgate over the entire descent. Given a drift-free gyro signal, sine and cosine components of fluxgate errors could be determined by least-squares. Finally, a complimentary smoothing filter was applied to the corrected gyro and corrected fluxgate that heavily favored the corrected gyro. Any systematic offset of the fluxgate (for example, mechanical misalignment) could not be determined, although no evidence of such an error could be seen in overlapping segments of the final sonar map.

Despite careful alignment, errors in roll measurement are inevitable. While the roll sensor has repeatability of 0.1 degree or better, several mechanical and electrical offsets arise between the measurement and the actual roll angle of the scanning sonar head. This error was determined by gathering sonar data while performing a slow heading spin when the vehicle rested on its descent mooring shortly after reaching the bottom. Roll error was deduced by examining the bottom profiles when the vehicle was at reciprocal headings. A nonlinear minimization technique was employed to determine the value of the roll bias that produced the most consistent composite profile using scans from both reciprocal headings.

Next, the sonar range and bearing measurements for each transect were transformed into world coordinates. This process involves first interpolating the navigation, attitude, and sonar data onto a

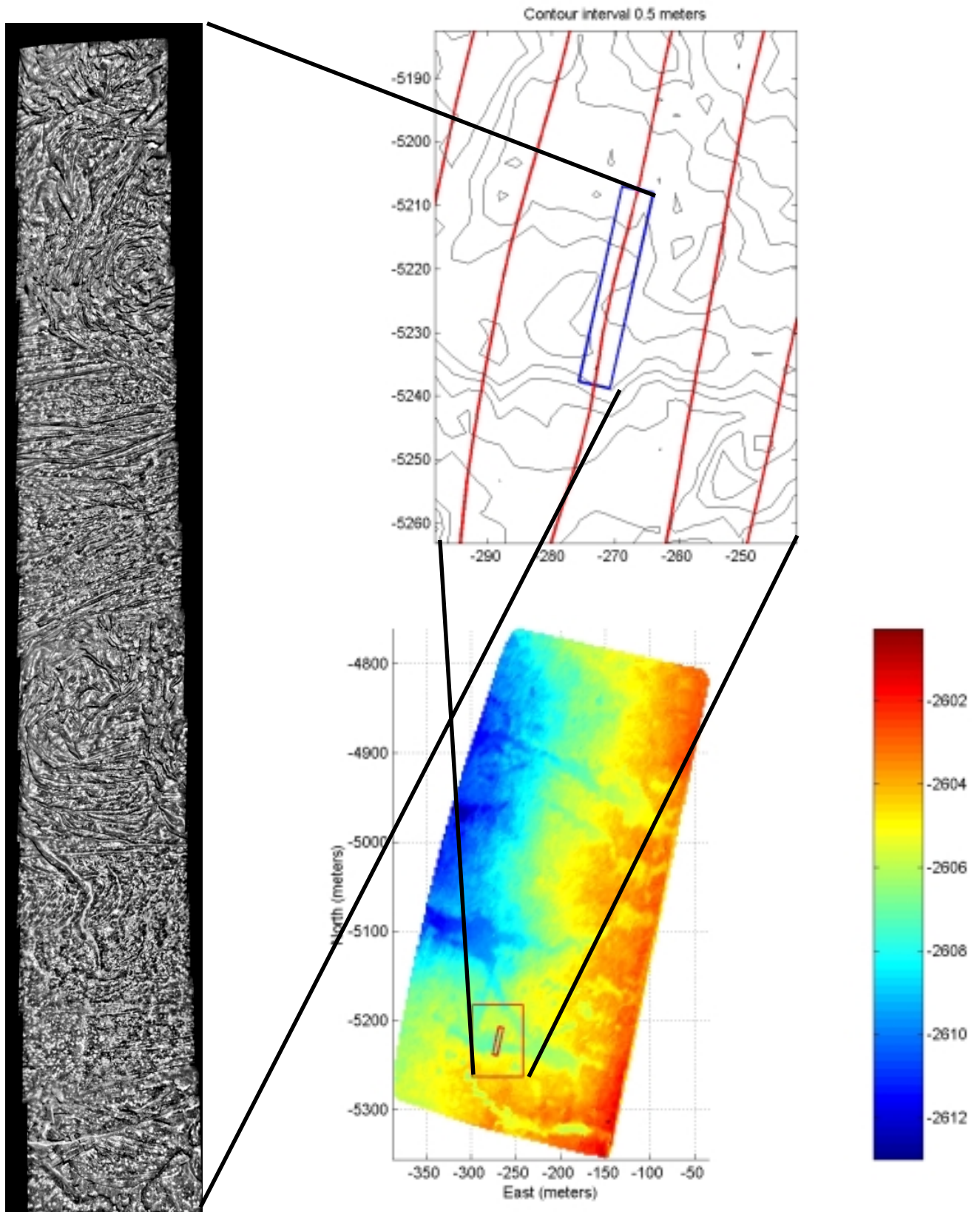


Figure 4. These plots show details of the coregistered sonar and video data. The lower right plot shows shaded bathymetry for the northern video survey area. The upper right plot shows contours (interval = 0.5 meters) surrounding an area shown in the video mosaic on the left

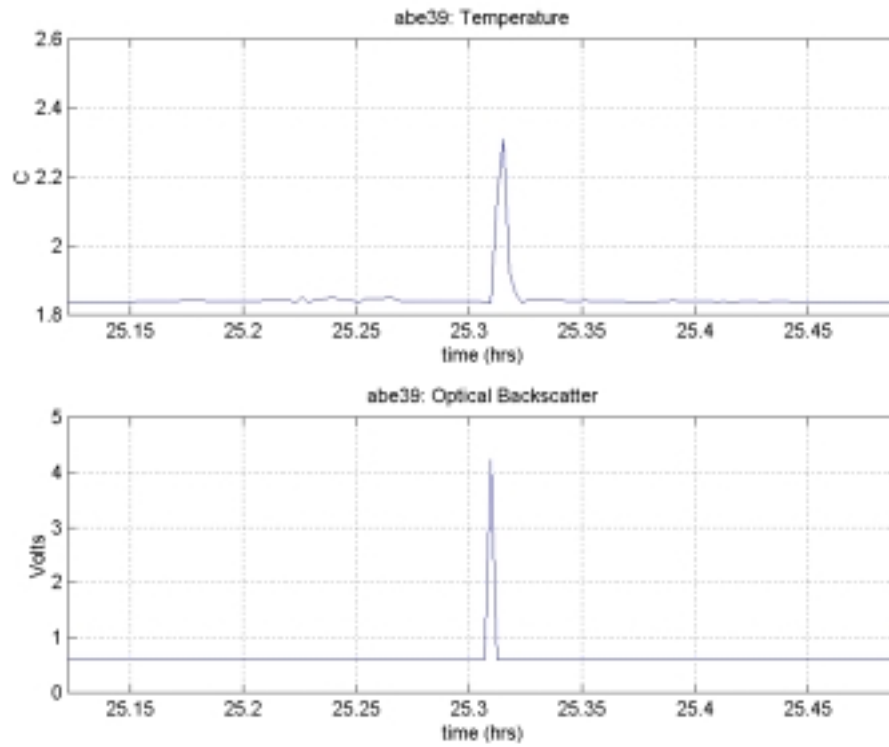


Figure 5. These plots show the temperature and optical backscatter readings as ABE passed over active hydrothermal vent

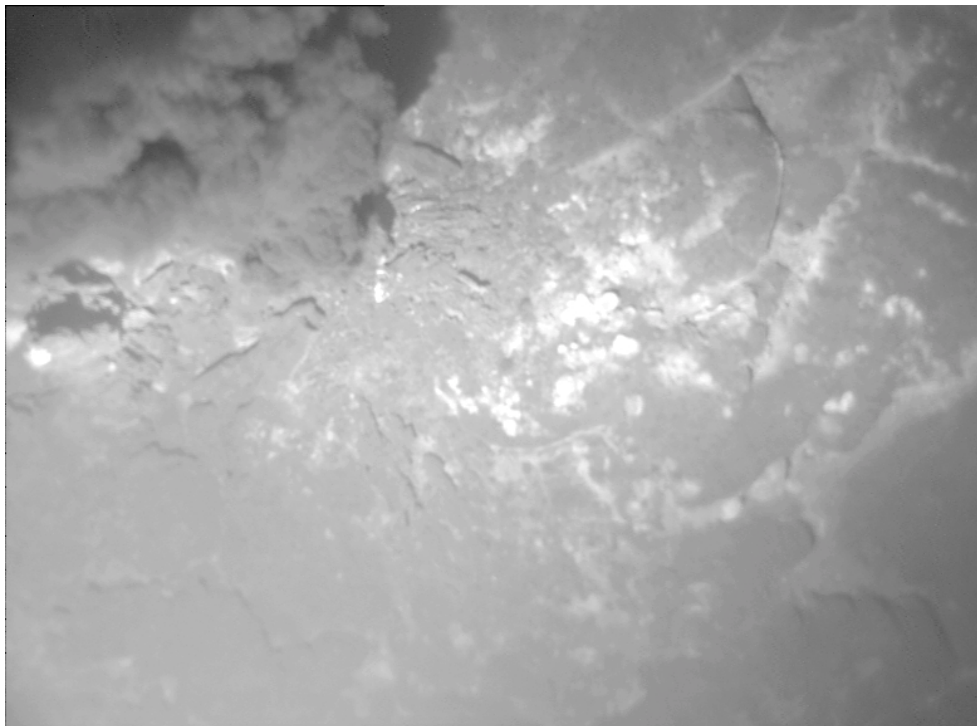


Figure 6. This video snapshot was taken shortly before the spikes in Figure 5 occurred. Billowing hydrothermal fluid can be seen in the upper left hand corner

common timebase, then transforming the sonar data from sensor into vehicle coordinates, and finally into world coordinates. Sonar measurements falling outside a prescribed range window were rejected.

The data from the scanning sonar (Imagenix 675kHz pencil-beam) required no interactive editing. While we experienced many missed returns in early runs (20 %), after increasing gain parameters gradually between runs, fewer than 1% of returns were missed in the later dives. The design of the sonar and the low acoustic and electrical noise levels of ABE all contributed to this result.

3.2 Bathymetry Results

Following the creation of individual sonar returns in world coordinates (the “dot cloud”), the data was gridded. Standard GMT [5] routines were employed. Figure 3 shows the results of the sonar survey in the northern area. The upper left plot in figure 3 shows the tracklines from the eight individual dives in the area. The bulk of the tracklines were devoted to overlapping sonar coverage, with the vehicle distance off the seafloor set to 20 meters. These tracks were spaced at 30 meters in early runs, we later increased the spacing to 40 meters. Other tracks were flown lower (5 meters off bottom) for video coverage. Some video lines ran up specific features, while other implemented a close grid spaced at 15 meters in the north west section of the area.

The upper right plot shows a shaded representation of the gridded bathymetry for the northern area, while the two lower plots show the slope and the relief. The relief plot utilizes a spatial high-pass filter to remove the long-scale changes in the terrain, highlighting the features on a scale of several tens of meters and smaller. These lower two plots, the slope and the relief, are useful for geological interpretation and also highlight the overall integrity of the data set. As both types of processing involve spatial differentiation, they would illuminate any mismatch between passes. These results were achieved using only the navigation and attitude corrections outlined earlier. No empirical matching of tracklines was required.

4. Coregistered Data Sets

Precise navigation and trackline control combined with the low acoustic and electrical noise of AUVs make them ideal platforms for gathering multisensor, coregistered data sets. On this cruise, we gathered the following scientific sensor data at all times:

- * Conductivity, Temperature
- * Optical Backscatter
- * Scanning sonar, Precision altimeter
- * 3-axis magnetometer

Additionally, ABE gathered video snapshots when programmed to fly at the appropriate height off bottom (approximately 5 meters). For several early dives, we had a pair of video cameras running which provided stereo image pairs. Unfortunately one camera was damaged on the fourth dive (during a rough launch), so we had only one camera for the remaining dives.

Our first example illustrates ABE’s capability for combined optical and sonar survey. In the upper section of the northern area, we programmed ABE to execute 15 meter-spaced tracklines while flying at video height. Over two dives (which also covered other areas), ABE covered an area comprising

250 meters by 500 meters in size. These tracks provided nearly 100% scanning sonar coverage and approximately 50% video coverage. Video images were taken at 5 second intervals, which provided approximately 20% overlap between images along-track.

Figure 4 shows a shaded bathymetric rendering of the sonar map over the northern video area, a video mosaic from a small section about 40 meters long, and a zoomed contour view showing the mosaic area in detail. The video mosaic was built using techniques developed at WHOI's Deep Submergence Laboratory that have been applied to a variety of geological, archaeological, and shipwreck forensics problems [9]. Although requiring extensive operator input, these techniques blend the images and allow the effects of uneven lighting and parallax to be reduced.

A second example of a coregistered data set involves the detection and confirmation of hydrothermal activity. On dive ABE 39, we programmed the vehicle to make video runs along specific features identified from previous sonar runs, including several crossings of the main summit trough (the "Crack of Doom"). This run also included the first half of the 15 meter spaced video survey shown in the previous example.

Figure 5 shows plots of temperature and optical backscatter as the vehicle passed over an active black smoker vent. Figure 6 shows the corresponding video snapshot, which provides confirmation that ABE detected an active vent plume. The upper left corner of the photo shows a "smoke" cloud.

5. Sampling with ABE

A maneuverable AUV such as ABE can be used for simple sampling tasks. After observing our colleagues sampling volcanic glass using a device called a wax core lowered to the seafloor using the ship's winch and wire, we decided to try taking such a sample from ABE. Wax coring works by crashing a heavy weight into the seafloor that has sticky wax on the bottom. The glass shatters due to the impact of the core and becomes trapped in the wax. These samples typically contain a few grams of glass, which is sufficient for detailed chemical analysis by laboratory instruments such as a mass spectrometer.

The actual sampling device was very simple. We mounted an aluminum tube protruding about .7 meters below the vehicle. A cylinder of wax was placed on the tip of the tube. Figure 7 shows the tube mounted on ABE along with the resulting sample of volcanic glass.

To take the core, we utilized ABE's ability to maneuver and the flexibility of its control system. Using existing commands, we were able to program ABE to stop, turn off its depth and trackline control, drive itself down for a prescribed period, twist, drive up, then reengage the depth and trackline control and continue along its desired track. The entire operation was performed open-loop based on timed sequences.

In addition to the sample, we obtained a detailed record of the sampling process and the surrounding seafloor. Due to the precision of ABE's navigation, we allowed the investigator to choose the precise location for the sample, we placed the sample correctly in the sonar map, and we obtained a set of video snapshots before, during, and after the sample was taken.



Figure 7. We utilized ABE’s controllability to take samples of volcanic glass using a wax-coring technique. We programmed ABE to stop at a selected spot, power down for a preset time, twist, then power up. The end of the core pole shattered glass on impact, and shards became trapped in the wax. A version that sequenced two poles (shown here) provided two samples per dive. The entire sampling sequence was captured on video still images

Following the success of our single wax core, we implemented a two core setup. Using a programmed “burn wire” release, bungee cords, and some nylon line, ABE could retract the first pole after taking a core and flip a second pole into the proper position to take another core. This device worked well and on our final dive we obtained two good samples.

6. Conclusion

The Autonomous Benthic Explorer (ABE) of the Woods Hole Oceanographic Institution acquired an extremely high resolution near-bottom dataset of bathymetry, magnetics, temperature, optical backscatter, conductivity, and digital video imaging along and across the narrow neovolcanic and active tectonic zone of the southern East Pacific Rise (17° to 19°S) during a total of 19 individual nighttime deployments of cruise AT3-31 of the Research Vessel Atlantis.

We significantly improved the robustness and precision of ABE’s long baseline acoustic navigation capability. These improvements resulted in better real-time control of the vehicle and helped produce superior mapping products. Specific upgrades included dynamic range-gating to eliminate surface

bounce returns and an additional transponder survey phase using acoustic travel-times gathered at the vehicle.

ABE's pencil-beam scanning sonar provided an echo-sounding capability unprecedented at this scale in tight coverage (2x5 m footprint) and the detail of measured relief. Gridded contours at 50 cm resolution produced a convincing picture of individual fault scarps, fissures, lava mounds, collapse pits, summit troughs, breached lava tubes, open-lava channels and lava pillars. Maps of seabed slopes define important details of the lava flows and the lack of trackline artifacts attest to the internal integrity of the data set.

Over subsets of the sonar coverage, ABE also obtained video snapshot coverage that has been assembled into mosaics and stereo pairs. These images provided ground-truth for the sonar bathymetry and provide a higher level of detail.

The temperature and optical backscatter probes discovered hot-water vents, with some collaborated by video images. In addition, we tested the feasibility of recovering basalt glasses with ABE. All three trials successfully recovered rock core samples, and each one is fully documented with video snapshots of the seafloor.

Acknowledgements

We would like to thank Dr. John Sinton for inviting us on his cruise and sharing the nighttime operations with us. Capt. George Silva and the crew of RV Atlantis performed flawlessly, launching and recovering ABE in difficult weather conditions. The WHOI Deep Submergence Operations Group (Dudley Foster, Expedition Leader) provided excellent support and advice during difficult moments. Our nighttime partners, Dr. Rodey Batiza and Eric Bergmanis, made sure each night operation yielded the maximum amount of data for everyone. Al Duester built the video system, made it perform well in the field, and attended to ABE's electrical systems. Rod Catanach took care of ABE's mechanical systems and invented the wax coring system at-sea in collaboration with Dr. Batiza. Anjana Shah and Wen Jin processed ABE data, including the bathymetry plots that appear in this paper. Dr. Hanumant Singh assembled the mosaic, which exceeded all our expectations. Our thanks go to Dr. Louis Whitcomb and Grey Lerner for their bathymetry software. This work was supported by NSF grants OCE-9216775 and OCE-9730813. This paper is WHOI contribution number 9980.

References

1. Tivey, M.A., Johnson, H.P., Bradley, A. and Yoerger, D., Thickness of a submarine lava flow determined from near-bottom magnetic field mapping by autonomous underwater vehicle, *Geophysical Research Letters*, Vol. 25, No. 6, pp. 805-808, March 1998.
2. Yoerger, D.R., Bradley, A., Walden, B., Singh, H. and Bachmayer, R., Surveying a subsea lava flow using the Autonomous Benthic Explorer (ABE), *Journal of the Japan Society for Marine Surveys and Technology*, Vol. 9, No. 1, pp. 43-60, March 1997.
3. Press, W., Flannery, B.P., Teuklosky, S.A., Vetterling, W.T., *Numerical Recipes in C*, Cambridge Press, 1988.
4. Watson, D.F, *Contouring, a guide to the analysis and display of spatial data*, Pergamon Press, 1992.
5. Wessel, P. and W. H. F. Smith, Free software helps map and display data, *EOS Trans. AGU*, 72, 441, 1991

6. Lerner, G., Whitcomb, L., Acoustic micro-bathymetry data processing and rendering software: Release notes for version 2, Technical Report, Dynamical Systems and Control Laboratory, Department of Mechanical Engineering, Johns Hopkins University, 1999
7. Ballard, R.D., The Jason-Medea remotely operated vehicle system, Deep Sea Research, Vol 40, No. 8, pp. 1673-1687, 1993.
8. Ballard, R.D, McCann, A.M., Yoerger, D.R., Whitcomb, L., Mindell, D., Oleson, J., Singh, H., Foley, B., Adams, J., Piechota, D., The Discovery of ancient history in the deep sea using advanced deep submergence technology, Deep Sea Research, to appear.
9. Howland, J., Singh, H., Marra, M., and Potter, D., Digital mosaicking of underwater imagery, Sea Technology, Vol 40 no. 6, June 1999.